Stability Analysis of the Continuum Based Constrained Mixture Model for Vascular Growth and Remodeling

Jiacheng Wu Shawn C. Shadden

Mechanical Engineering, University of California, Berkeley, CA, United States

Abstract

A stabilizing criterion is derived for the equations governing vascular growth and remodeling. We start from the integral state equations of the continuum based constrained mixture theory of vascular growth and remodeling and obtain a system of time-delayed differential equations describing vascular growth. By employing an exponential form of the constituent survival function, the delayed differential equations can be reduced to a nonlinear ODE system. Linear analysis shows that the homeostatic state is a degenerate fixed point, which precludes application of linear stability conclusions to the nonlinear system. To resolve this problem, a sub-system is constructed by recognizing a linear relation between two states. Subsequently Lyapunov's indirect method is used to connect stability properties between the linearized system and the original nonlinear system. This analysis leads to a stability criterion for vascular expansion in terms of growth and remodeling kinetic parameters, geometric quantities and material properties. Numerical simulations were conducted to verify the stability conclusions from the theoretical analysis, as well as study the influence key parameters on growth properties. The theoretical results are also compared with prior numerical and experimental findings in the literature.

1 Introduction

The functional adaptation of arteries to biomechanical stimuli has been long recognized as an important feature of vascular growth and remodeling (G&R), and has led to the development of mathematical theories to describe such phenomena [16]. A common theoretical framework has been the constrained mixture theory model for studying growth and remodeling of soft tissues [18]. Previous research in applying the constrained mixture theory of vascular G&R has focused mostly on numerical investigations, and especially in relation to aneurysm growth. For example, [4, 5] applied the constrained mixture theory to study stress mediated aneurysm expansion in idealized geometries to better understand different factors influencing geometry and aneurysm growth rate. Later, G&R theory was extended to more 3D geometries to predict complex aneurysm shapes [29]. In addition, vascular G&R simulations have been coupled with blood flow dynamics to study the coupling between hemodynamics (e.g. wall shear stress) and aneurysm formation and growth in cylindrical-type geometries [13, 26, 23], and more recently to patient-specific geometries [28].

It has been suggested [6, 3] that a better understanding for risk of aneurysm rupture may involve the stability of aneurysm expansion due to vascular G&R, i.e., rupture might be a result of unstable vascular G&R. While the above studies considered the numerical implementation of G&R in various

applications, theoretical analysis of the stability of the underlying adaptive mechanism has received less attention. In this regard, the recent work of [21] studied the arterial growth instability using a goal function based approach. In addition, [9, 10] defined the concept of mechanobiological stability based on a Lyapunov analysis of differential equations of mass density and vessel wall position. The above analyses do not explicitly account for the dependence of the total strain energy on the history of the growth, which may be an important consideration in the constrained mixture theory of vascular G&R. Moreover, stability properties for the constrained mixture model for G&R have yet to be established rigorously. As demonstrated herein, linear stability analysis as proposed in prior works, to study the stability of the homeostatic state cannot be directly applied to infer the stability of the original (nonlinear) system due to the degenerate nature of the homeostatic state. In this work, we start from the integral state equations of the continuum based constrained mixture model of G&R and derive the state equations (time-delayed differential equations) describing the progression of aneurysm expansion. By employing a commonly used exponential form of the constituent survival function and introducing an extended state variable , the delayed differential equations can be reduced to an ODE system. Linear stability analysis is subsequently applied to this ODE system and a stability criteria is obtained based on G&R kinetic parameters and material properties. To address the problem of the degeneracy of the linearized system about the homeostatic state mentioned above, we formulate a reduced sub-system that is shown to be exponentially stable, which enables us to extend the linear stability results to the original (nonlinear) system and rigorously prove stability properties observed in prior computational and theoretical studies.

2 Constrained mixture theory of growth and remodeling

The vessel wall has the ability to adapt to changes of mechanical environment to maintain a homeostatic state via vascular G&R [16, 24]. This process occurs through removal of old vascular constituents and incorporation of new constituents, which can be described by an equation of the form

$$M(t) = M(0)Q(t) + \int_0^t m(\tau)q(t-\tau)d\tau \ . \tag{1}$$

$M(t)$ is the mass per unit area of vascular constituents at time t. The first term on the right represents the contribution from the "initial" mass before G&R, whereas the second term on the right represents the incorporation and natural turnover of newly produced constituent. Specifically, $Q(t)$ is the remaining fraction of initial mass at the current time t, $m(\tau)$ is the mass production rate of vascular constituent at time τ, and $q(t-\tau)$ is the remaining fraction of newly produced constituent at time t.

The mass production rate $m(t)$ is assumed to depend linearly on the deviation of wall tension σ with respect to a homeostatic stress σ_h [5],

$$m(t) = M(t)\left[k_g[\sigma(t) - \sigma_h] + f_h\right] \tag{2}$$

where k_g is the growth feedback constant and f_h is the basal value of the mass production rate. The above growth law describes the stress-mediated feedback mechanism by which the homeostatic stress is maintained.

In the constrained mixture theory of G&R [18], the vessel wall is modeled as a membrane and treated as a constrained mixture, i.e., all vascular constituents deform together at each location.

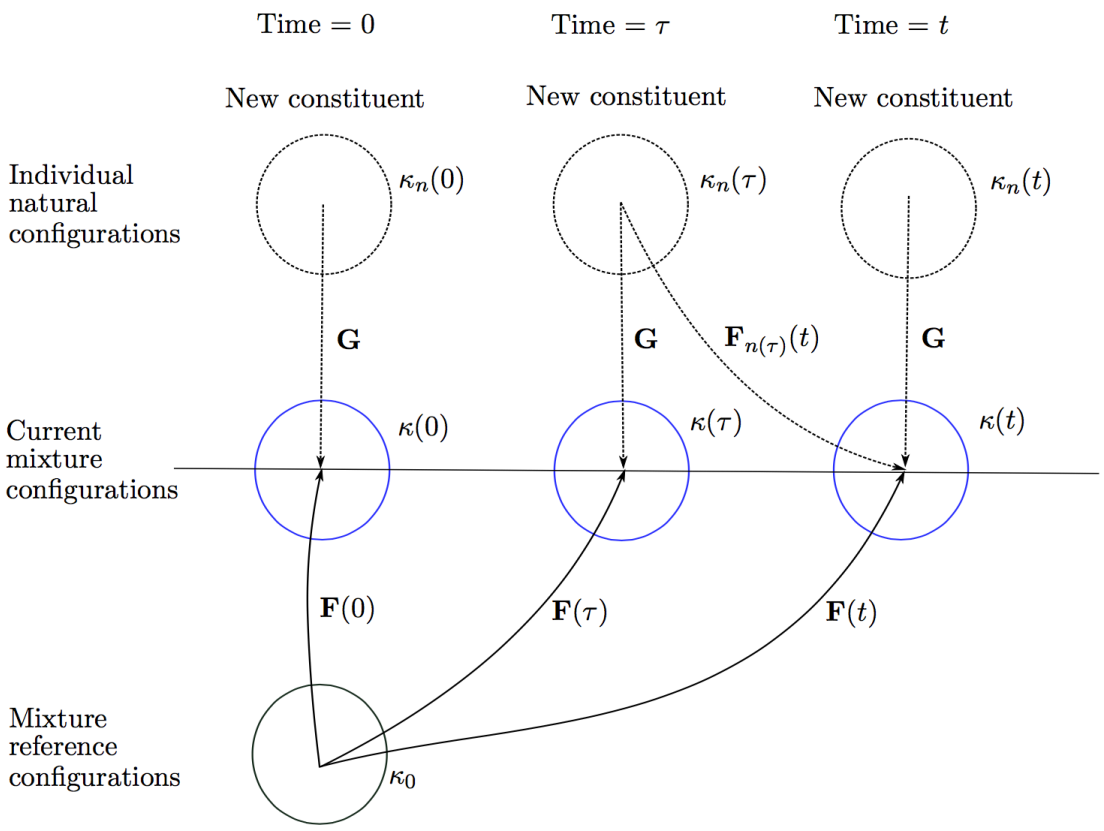

Figure 1: Configurations and associated mappings used to describe G&R framework.

The reference configuration κ_0 for the vascular mixture corresponds to the configuration with zero transmural pressure. For any time t, the current configuration of the mixture is denoted as $\kappa(t)$, and $\mathbf{F}(t)$ is the deformation gradient tensor mapping from κ_0 to $\kappa(t)$. However, the deformation of individual vascular constituents is computed with respect their natural configurations $\kappa_{n(\tau)}$, which is characterized by the time τ when the constituent was produced. The newly produced vascular constituent is deposited into the vascular mixture with pre-stretch defined by $\mathbf{G}(\tau)$, which maps from the natural configuration $\kappa_{n(\tau)}$ to the deformed configuration of the mixture at τ. Therefore, based on the relations between different configurations shown in Figure 1, the deformation gradient tensor of the vascular constituents produced at time τ mapping from the natural configuration $\kappa_{n(\tau)}$ to the current deformed configuration $\kappa(t)$ is defined as

$$\mathbf{F}_{n(\tau)}(t) = \mathbf{F}(t)\mathbf{F}^{-1}(\tau)\mathbf{G}(\tau)\ . \tag{3}$$

Therefore, the right Cauchy-Green deformation tensor is computed as

$$\mathbf{C}_{n(\tau)}(t) = \mathbf{F}_{n(\tau)}(t)^T\mathbf{F}_{n(\tau)}(t)\ . \tag{4}$$

The pre-stretch tensor $\mathbf{G}(\tau)$ is defined as two-point tensor

$$\mathbf{G}(\tau) = G_h \mathbf{e}(\tau) \otimes \mathbf{e}_{n(\tau)} \ , \tag{5}$$

where $\mathbf{e}(\tau)$ is the direction of vascular constituent at time τ in the mixture configuration $\kappa(\tau)$ and $\mathbf{e}_{n(\tau)}$ is the direction of the vascular constituent produced at time τ in its natural configuration, $\kappa_{n(\tau)}$. The relation between $\mathbf{e}(\tau)$ and $\mathbf{e}_{n(\tau)}$ is described by

$$\mathbf{e}_{n(\tau)} = \frac{\mathbf{G}(\tau)^{-1}\mathbf{e}(\tau)}{\|\mathbf{G}(\tau)^{-1}\mathbf{e}(\tau)\|} \ . \tag{6}$$

G_h is the pre-stretch of the vascular constituent when it is deposited into the mixture, and since we assume it is equal to the stretch ratio of vascular constituent in the homeostatic state, we mark it using the subscript "h".

After $\mathbf{C}_{n(\tau)}(t)$, $\mathbf{G}(\tau)$ and $\mathbf{e}_{n(\tau)}$ are defined, the stretch ratio of the vascular constituent produced at time τ with respect to its natural configuration $\kappa_{n(\tau)}$ can be computed as

$$\begin{aligned}
\lambda_{n(\tau)}(t) &= \sqrt{\mathbf{e}_{n(\tau)} \cdot \mathbf{C}_{n(\tau)}(t)\mathbf{e}_{n(\tau)}} \\
&= \left\|\mathbf{F}(t)\mathbf{F}^{-1}(\tau)\mathbf{G}(\tau)\mathbf{e}_{n(\tau)}\right\| \\
&= \left\|\mathbf{F}(t)\mathbf{F}^{-1}(\tau)G_h\left(\mathbf{e}(\tau)\otimes\mathbf{e}_{n(\tau)}\right)\mathbf{e}_{n(\tau)}\right\| \\
&= G_h\left\|\mathbf{F}(t)\mathbf{F}^{-1}(\tau)\mathbf{e}(\tau)\right\| \\
&= G_h\frac{\left\|\mathbf{F}(t)\mathbf{F}^{-1}(\tau)\mathbf{e}(\tau)\right\| / \left\|\mathbf{F}^{-1}(\tau)\mathbf{e}(\tau)\right\|}{\|\mathbf{e}(\tau)\| / \|\mathbf{F}^{-1}(\tau)\mathbf{e}(\tau)\|} \\
&= G_h\frac{\lambda(t)}{\lambda(\tau)} \ ,
\end{aligned} \tag{7}$$

where $\lambda(t)$ is the stretch ratio of mixture in the direction of vascular constituents, defined as

$$\lambda(t) = \frac{\left\|\mathbf{F}(t)\mathbf{F}^{-1}(\tau)\mathbf{e}(\tau)\right\|}{\|\mathbf{F}^{-1}(\tau)\mathbf{e}(\tau)\|} \ . \tag{8}$$

Based on the mass-averaged principle for a constrained mixture, the total strain energy per unit area for the mixture at current time t is

$$W(t) = \frac{M(0)}{\rho}Q(t)\hat{W}(\lambda_{n(0)}(t)) + \int_0^t \frac{m(\tau)}{\rho}q(t-\tau)\hat{W}(\lambda_{n(\tau)}(t))d\tau \ , \tag{9}$$

where ρ is the volume density of the vessel wall and $\hat{W}$ denotes the strain energy per unit volume and depends on the stretch ratio $\lambda_{n(\tau)}(t)$. The mathematical form of $\hat{W}$ is determined by the constitutive relation.

Our goal is to perform stability analysis of vascular G&R. To simplify the analysis while retaining the essential dynamics, we assume the geometry is cylindrical and deformation occurs in the radial direction, as aneurysm progression is mostly characterized by radial expansion. We further assume that vascular constituents align in the circumferential direction to sustain the radial expansion; this assumption is not significant since for constituents that are not aligned in the circumferential direction we can consider their circumferential projected components.

Under these assumptions, the stretch ratio of the mixture in the circumferential direction, $\lambda_{circ}(t)$, is obtained as

$$\lambda_{circ}(t) = \frac{\left\|\mathbf{F}(t)\mathbf{F}^{-1}(\tau)\mathbf{e}_{circ}\right\|}{\left\|\mathbf{F}^{-1}(\tau)\mathbf{e}_{circ}\right\|} = \frac{r(t)}{R} \,, \tag{10}$$

where $r(t)$ is the vessel radius at time t in the mixture configuration $\kappa(t)$ and R is the vessel radius in the mixture reference configuration κ_0. Hence, the stretch ratio of the vascular constituents with respect the natural configuration is obtained as

$$\lambda_{n(\tau)}(t) = G_h \frac{\lambda_{circ}(t)}{\lambda_{circ}(\tau)} = G_h \frac{r(t)}{r(\tau)} \,. \tag{11}$$

While constitutive relations of vascular material are often nonlinear [14, 17], we herein assume a linearized stress-strain relation with respect the homeostatic states of the vessel wall for the purpose of stability analysis. Therefore, if the vascular material is assumed linear, and expansion is radial,

$$\hat{W}(\lambda_{n(\tau)}(t)) = \frac{1}{2}E\left[\lambda_{n(\tau)}(t) - 1\right]^2 = \frac{1}{2}E\left[G_h\frac{r(t)}{r(\tau)} - 1\right]^2 \,, \tag{12}$$

where $\lambda_{n(\tau)}(t) - 1$ represents the strain of the vascular constituents with respect their natural configurations $\kappa_{n(\tau)}$. Therefore (9) becomes

$$W(t) = \frac{M(0)}{\rho}Q(t)\frac{1}{2}E\left[G_h\frac{r(t)}{r_h} - 1\right]^2 + \int_0^t \frac{m(\tau)}{\rho}q(t-\tau)\frac{1}{2}E\left[G_h\frac{r(t)}{r(\tau)} - 1\right]^2 d\tau \,, \tag{13}$$

where r_h is initial homeostatic value for vessel radius. Note that for the initial mass, the stretch ratio is equal to $G_h\frac{r(t)}{r_h}$ instead of $G_h\frac{r(t)}{r(0)}$ because the initial vascular constituents are not necessarily produced at $t = 0$, instead they are produced when the vessel radius equals to r_h since we assumed G&R is in the homeostatic state before $t = 0$.

Since we are interested in stability (i.e., long term behavior) we can ignore the initial condition terms in both (1) and (13) as these terms will decay to zero, and we are left with

$$M(t) = \int_0^t m(\tau)q(t-\tau)d\tau \tag{14}$$

$$W(t) = \int_0^t \frac{m(\tau)}{\rho}q(t-\tau)\frac{1}{2}E\left[G_h\frac{r(t)}{r(\tau)} - 1\right]^2 d\tau \,. \tag{15}$$

In the case of cylindrical geometry, the force balance equation in the circumferential direction yields

$$Pr(t) = T_\theta(t) = \frac{1}{\lambda_z(t)}\frac{\partial W(t)}{\partial \lambda_\theta(t)} \,, \tag{16}$$

where

$$\lambda_z = 1, \quad \lambda_\theta(t) = \frac{r(t)}{R} \,. \tag{17}$$

Therefore,

$$\frac{\partial W(t)}{\partial \lambda_\theta} = R\frac{\partial W(t)}{\partial r(t)} = R\int_0^t \frac{m(\tau)}{\rho}q(t-\tau)E\left[G_h\frac{r(t)}{r(\tau)} - 1\right]\frac{G_h}{r(\tau)}d\tau. \tag{18}$$

Substituting the above into (16) yields

$$Pr(t) = R\int_0^t \frac{m(\tau)}{\rho} q(t-\tau) E\left[G_h \frac{r(t)}{r(\tau)} - 1\right] \frac{G_h}{r(\tau)} d\tau \ . \tag{19}$$

Note that mean arterial pressure is used here and is assume to be constant. We ignore the pulsatility of the pressure through the cardiac cycle because we are interested in the long term behavior of vascular G&R.

3 Converting to an ODE system

From the previous section, the time evolution of vascular growth and remodeling is modeled by the following equations

$$\begin{aligned} M(t) &= \int_0^t m(\tau) q(t-\tau) d\tau \ , & (20)\\ Pr(t) &= R\int_0^t \frac{m(\tau)}{\rho} q(t-\tau) E\left[G_h \frac{r(t)}{r(\tau)} - 1\right] \frac{G_h}{r(\tau)} d\tau \ , & (21)\\ m(t) &= M(t)\left[k_g[\sigma(t) - \sigma_h] + f_h\right] \ , & (22)\\ \sigma(t) &= \frac{Pr(t)}{h(t)} \ , & (23) \end{aligned}$$

where $h(t) = \frac{M(t)}{\rho J(t)}$ is the vessel wall thickness, and J is the determinant of the deformation gradient tensor, which is equal to $\frac{r(t)}{R}$. Equation (23) is the Laplace law for wall tension in the circumferential direction. Since the current behavior of the system depends continuously on all past time history, the system is a continuous time-delayed system. For analysis, it is convenient if we can convert this to an ODE system depending on current states. To make this reduction possible, we assume the survival function has an exponential decay

$$q(t) = \exp(-\alpha t) \ , \tag{24}$$

where $\alpha > 0$ is the decaying constant. This implies that the rate of decay of the constituent is proportional to its current value as

$$\dot{q}(t) = -\alpha q(t). \tag{25}$$

To proceed we differentiate (20) with respect to t

$$\begin{aligned} \dot{M}(t) &= m(t) - \alpha \int_0^t m(\tau) q(t-\tau) d\tau & (26)\\ &= m(t) - \alpha M(t). & (27) \end{aligned}$$

Substituting in (22) yields

$$\dot{M}(t) = M(t) k_g \left[\sigma(t) - \sigma_h\right] + M(t)\left[f_h - \alpha\right]. \tag{28}$$

Since f_h is the basal value of the mass production rate, it should balance with the natural decay of constituents caused by the survival function $q(t)$. Thus we require that $f_h = \alpha$ and subseqently

$$\dot{M}(t) = M(t) k_g \left[\sigma(t) - \sigma_h\right] \ . \tag{29}$$

Now taking the time derivative of (21) yields

$$\begin{aligned} P\dot{r}(t) &= R\left[\frac{m(t)}{\rho}E\left(G_h-1\right)\frac{G_h}{r(t)}\right. \\ &+\int_0^t \frac{m(\tau)}{\rho}q(t-\tau)E\,G_h\frac{\dot{r}(t)}{r(\tau)}\frac{G_h}{r(\tau)}d\tau \\ &\left.-\alpha\int_0^t \frac{m(\tau)}{\rho}q(t-\tau)E\left[G_h\frac{r(t)}{r(\tau)}-1\right]\frac{G_h}{r(\tau)}d\tau\right]\ . \end{aligned} \tag{30}$$

The last term in the above equation is just $-\alpha Pr(t)$, and defining an extended state variable

$$y(t) = R\int_0^t \frac{m(\tau)}{\rho}q(t-\tau)E\frac{G_h^2}{r^2(\tau)}d\tau \tag{31}$$

yields

$$\dot{r}(t) = \frac{m(t)}{r(t)}\frac{RE\left[G_h-1\right]G_h}{P\rho} + \frac{1}{P}y(t)\dot{r}(t) - \alpha r(t)\ . \tag{32}$$

Take time derivative of (31), we obtain the ODE characterizing dynamics of $y(t)$

$$\dot{y}(t) = k_2\frac{m(t)}{r^2(t)} - \alpha y(t)\ . \tag{33}$$

where $k_2 = \frac{G_h^2 ER}{\rho}$. The extended state y represents the generalized stiffness of the vascular mixture, as explained later in the Discussion section.

Based on (22), (23), (29), (32) and (33), the system of equations for vascular growth can now be written as

$$\dot{M}(t) = M(t)k_g\left[\sigma(t)-\sigma_h\right] \tag{34}$$

$$\dot{r}(t) = \frac{1}{k(t)}\left[\alpha r(t) - \frac{m(t)}{r(t)}k_1\right] \tag{35}$$

$$\dot{y}(t) = k_2\frac{m(t)}{r^2(t)} - \alpha y(t) \tag{36}$$

$$m(t) = M(t)\left[k_g\left[\sigma(t)-\sigma_h\right]+f_h\right] \tag{37}$$

$$\sigma(t) = \frac{\rho Pr(t)^2}{M(t)R} \tag{38}$$

where $k(t) = \frac{1}{P}y(t) - 1$, $k_1 = \frac{RE[G_h-1]G_h}{P\rho}$ and $f_h = \alpha$.

4 Stability analysis of the ODE system

4.1 Linearization of state equations

The stability of vascular growth is characterized by the stability of the ODE system we obtained in previous section. To analyze its stability, we examine the nature of the linearized system about the homeostatic state. Namely, we assume the vessel wall is initially in its homeostatic state before

G&R is introduced by whatever cause. Mass density and vessel radius in the initial homeostatic state are denoted M_h and r_h respectively. Strictly speaking, as shown later, there is no "homeostatic state" for mass density $M(t)$ and $r(t)$ because asymptotic stability does not hold for $M(t)$ and $r(t)$. However, for convenience, we use the term "homeostatic state" to denote the asymptotic states M_h and r_h.

Based on (38), the homeostatic value of circumferential stress σ_h is

$$\sigma_h = \frac{\rho P r_h^2}{M_h R} \; . \tag{39}$$

Substituting homeostatic values into (32) yields

$$\frac{\rho P r_h}{M_h} = E\left[G_h - 1\right] \; . \tag{40}$$

Combining (39) and (40) and observing $G_h = \frac{r_h}{R}$, we obtain an alternate expression for σ_h

$$\sigma_h = E\left[G_h - 1\right] G_h \; . \tag{41}$$

Similarly, substituting homeostatic values into (31) yields the homeostatic value for the extended state $y(t)$

$$y_h = \frac{REG_h^2 M_h}{\rho r_h^2} \; . \tag{42}$$

We next consider perturbation of the system around the homeostatic values above

$$\begin{aligned} M(t) &= M_h + \Delta M(t) && (43)\\ r(t) &= r_h + \Delta r(t) && (44)\\ y(t) &= y_h + \Delta y(t) && (45)\\ \sigma(t) &= \sigma_h + \Delta\sigma(t) && (46) \end{aligned}$$

with

$$\frac{\Delta M}{M_h},\ \frac{\Delta r}{r_h},\ \frac{\Delta y}{y_h},\ \frac{\Delta\sigma}{\sigma_h} \ll 1 \; . \tag{47}$$

To obtain the linearized equations, it is convenient to first obtain the first order approximation of $\Delta\sigma$

$$\begin{aligned} \Delta\sigma(t) &= \sigma(t) - \sigma_h \\ &= \frac{\rho P}{R}\left[\frac{[r_h + \Delta r]^2}{M_h + \Delta M} - \frac{r_h^2}{M_h}\right] \\ &\approx \frac{\rho P}{R}\left[\frac{2r_h}{M_h}\Delta r - \frac{r_h^2}{M_h^2}\Delta M\right] \; . \end{aligned} \tag{48}$$

Therefore, the linearized state equation for mass density $M(t)$ is obtained as

$$\begin{aligned} \Delta\dot{M} &= \dot{M} = Mk_g\Delta\sigma \\ &\approx [M_h + \Delta M]k_g\frac{\rho P}{R}\left[\frac{2r_h}{M_h}\Delta r - \frac{r_h^2}{M_h^2}\Delta M\right] \\ &\approx k_g\frac{\rho P}{R}\left[2r_h\Delta r - \frac{r_h^2}{M_h}\Delta M\right] \; . \end{aligned} \tag{49}$$

Similarly, we can obtain the linearized state equations for vessel radius $r(t)$ and generalized stiffness $y(t)$ as

$$\dot{\Delta r} \approx \frac{1}{k_h}\left[\left[2\alpha - \frac{2k_g r_h^2 \rho P}{RM_h}\right]\Delta r + \left[-\frac{\alpha r_h}{M_h} + \frac{k_g r_h^3 \rho P}{M_h^2 R}\right]\Delta M\right] \tag{50}$$

$$\dot{\Delta y} \approx -\frac{2k_2 M_h}{r_h^3}\left[\alpha - \frac{k_g \rho P r_h^2}{RM_h}\right]\Delta r - \frac{k_2}{r_h^2}\left[\alpha - \frac{k_g \rho P r_h^2}{RM_h}\right]\Delta M - \alpha \Delta y \tag{51}$$

where $k_h = \frac{1}{G_h - 1}$ and $k_2 = \frac{G_h^2 ER}{\rho}$.

Equations (49)–(51) describe the time evolution of the linearized variables $(\Delta M, \Delta r, \Delta y)$. We will first consider the linear stability of the subsystem for $(\Delta M, \Delta r)$. This is reasonable since the dynamics of Δr and ΔM are decoupled from the dynamics of Δy. Also, the time evolution of mass density M and vessel radius r are of paramount interest.

Based on (49) and (50), the linearized state equations for Δr and ΔM become

$$\begin{bmatrix} \dot{\Delta r} \\ \dot{\Delta M} \end{bmatrix} = \begin{bmatrix} A & B \\ C & D \end{bmatrix} \times \begin{bmatrix} \Delta r \\ \Delta M \end{bmatrix} \tag{52}$$

where

$$A = \frac{1}{k_h}\left[2\alpha - \frac{2k_g r_h^2 \rho P}{RM_h}\right], \tag{53}$$

$$B = \frac{1}{k_h}\left[-\frac{\alpha r_h}{M_h} + \frac{k_g r_h^3 \rho P}{M_h^2 R}\right], \tag{54}$$

$$C = \frac{2k_g \rho P r_h}{R}, \tag{55}$$

$$D = -\frac{k_g \rho P r_h^2}{RM_h}. \tag{56}$$

4.2 Stability of the linearized state equations

To determine whether G&R is stable, we need to first find the eigenvalues of system matrix. Let the characteristic polynomial for the system be equal to zero

$$\begin{vmatrix} A-\lambda & B \\ C & D-\lambda \end{vmatrix} = \lambda^2 - [A+D]\lambda + [AD - BC] = 0\,. \tag{57}$$

It can be verified that $AD - BC = 0$ based on (53)–(56). Therefore, the corresponding eigenvalues are

$$\lambda_1 = A + D, \quad \lambda_2 = 0\,. \tag{58}$$

This means $[\Delta r, \Delta M] = [0, 0]$ is a **degenerate** fixed point of the linearized system.

Theorem 4.1. (Neutrally Stable Fixed Point) *Consider an autonomous dynamical system* $\dot{\mathbf{x}} = \mathbf{A}\mathbf{x}$ *with system matrix*

$$\mathbf{A} = \begin{bmatrix} A & B \\ C & D \end{bmatrix} \tag{59}$$

whose eigenvalues are λ_1 *and* λ_2*. Let* $\tau = \mathrm{Tr}(\mathbf{A}) = A + D$*,* $\Delta = \det(\mathbf{A}) = AD - BC$*. If*

$$\Delta = 0, \quad \tau < 0 \tag{60}$$

then $\lambda_1 < 0$ *and* $\lambda_2 = 0$ *and there exists a line of neutrally stable non-isolated* **degenerate** *fixed points passing through* $\mathbf{x} = \mathbf{0}$*. A neutrally stable fixed point denotes a fixed point which is Lyapunov stable but not attracting.*

Based on Theorem 4.1, the neutrally stabilizing condition for the linearized system (52) at the fixed point $(\Delta r, \Delta M) = (0, 0)$ is $A + D < 0$, i.e.

$$k_g > \frac{\alpha R M_h}{\rho P r_h^2} \left[\frac{1}{1 + \frac{E M_h}{2 \rho P r_h}} \right] . \tag{61}$$

However, since the fixed point is degenerate, stability of hemostatic state for the nonlinear system cannot be inferred [25].

4.3 Avoiding the degeneracy condition

In order to avoid the degenerate fixed point problem encountered above, the 3-state linearized system is reconsidered

$$\frac{d}{dt} \begin{bmatrix} \Delta r \\ \Delta M \\ \Delta y \end{bmatrix} = \begin{bmatrix} \frac{1}{k_h} \left[\alpha - \frac{k_g \rho P r_h^2}{R M_h} \right] \left[2\Delta r - \frac{r_h}{M_h} \Delta M \right] \\ \frac{k_g \rho P r_h}{R} \left[2\Delta r - \frac{r_h}{M_h} \Delta M \right] \\ -\frac{k_2 M_h}{r_h^3} \left[\alpha - \frac{k_g \rho P r_h^2}{R M_h} \right] \left[2\Delta r - \frac{r_h}{M_h} \Delta M \right] - \alpha \Delta y \end{bmatrix} . \tag{62}$$

It can be observed that there is a linear relation between derivatives of Δr and ΔM,

$$\dot{\Delta r} = B_1 \dot{\Delta M} \tag{63}$$

where

$$B_1 = \frac{\left[\alpha - \frac{k_g \rho P r_h^2}{R M_h} \right] R}{k_h k_g \rho P r_h} , \tag{64}$$

which in fact is responsible for the degeneracy observed above. Note that B_1 is positive if

$$k_g < \frac{\alpha R M_h}{\rho P r_h^2} . \tag{65}$$

We can now integrate the derivative relation (63) from 0 to t to obtain

$$\Delta r(t) = B_1 \Delta M(t) + B_2 , \tag{66}$$

where constant B_2 only depends on initial conditions

$$B_2 = \Delta r(0) - B_1 \Delta M(0) . \tag{67}$$

Based on (66) and substituting Δr with ΔM, the 3-state system $(\Delta r, \Delta M, \Delta y)$ is reduced to a 2-state system of $(\Delta M, \Delta y)$

$$\frac{d}{dt}\begin{bmatrix} \Delta M \\ \Delta y \end{bmatrix} = \begin{bmatrix} \frac{k_g \rho Pr_h}{R}\left[2B_1 - \frac{r_h}{M_h}\right]\Delta M + \frac{2k_g \rho Pr_h}{R}B_2 \\ B_3 \dot{\Delta M} - \alpha \Delta y \end{bmatrix}, \tag{68}$$

where the constant B_3 is defined as

$$B_3 = -\frac{k_2\left[\alpha - \frac{k_g \rho Pr_h^2}{RM_h}\right]M_h R}{k_g \rho Pr_h^2}. \tag{69}$$

The linear system (68) is nonhomogeneous because of the constant term $\frac{2k_g \rho Pr_h}{R}B_2$ on the right hand side of the first equation. It can be shown that the above nonhomogeneous system is neutrally stable in the sense that the state variables $(\Delta M, \Delta y)$ remain bounded, while exponential stability cannot be obtained due to the nonhomogeneous term. However, in order to extend the stability conclusion from the linearized system to the original nonlinear system, exponential stability of the linearized system should be obtained. Therefore, we homogenize the linear system by taking the time derivative of the first equation in (68), yielding a homogeneous 2-state system for $(\dot{\Delta M}, \Delta y)$ as

$$\frac{d}{dt}\begin{bmatrix} \dot{\Delta M} \\ \Delta y \end{bmatrix} = \begin{bmatrix} \frac{k_g \rho Pr_h}{R}\left[2B_1 - \frac{r_h}{M_h}\right] & 0 \\ B_3 & -\alpha \end{bmatrix} \times \begin{bmatrix} \dot{\Delta M} \\ \Delta y \end{bmatrix}. \tag{70}$$

The eigenvalues for the system matrix of (70) are

$$\lambda_1 = \frac{k_g \rho Pr_h}{R}\left[2B_1 - \frac{r_h}{M_h}\right], \quad \lambda_2 = -\alpha. \tag{71}$$

Therefore the linear system is exponentially stable if and only if

$$\frac{k_g \rho Pr_h}{R}\left[2B_1 - \frac{r_h}{M_h}\right] < 0, \quad \alpha > 0 \tag{72}$$

By substituting (64) in to the inequalities above, the exponentially stability condition is given by

$$k_g > \frac{\alpha R M_h}{\rho Pr_h^2}\left[\frac{1}{1 + \frac{EM_h}{2\rho Pr_h}}\right] \triangleq k_{cr}, \quad \alpha > 0, \tag{73}$$

where k_{cr} denotes the critical value for the growth feedback constant k_g to ensure stability.

Theorem 4.2. (Lyapunov's Indirect Method) *Consider an autonomous nonlinear system* $\dot{\mathbf{x}} = \mathbf{f}(\mathbf{x})$ *with linearized system about* $\mathbf{x} = \mathbf{0}$ *(without loss of generality) as* $\dot{\mathbf{x}} = \mathbf{A}\mathbf{x}$*, where*

$$\mathbf{A} = \nabla \mathbf{f}(\mathbf{x})|_{\mathbf{x}=\mathbf{0}} \tag{74}$$

is the system matrix for the linear system. If the eigenvalues of matrix A satisfy

$$Re(\lambda_i) < 0, \quad \forall\ i = 1, 2, \ldots, \tag{75}$$

(i.e the linearized system is exponentially stable), then the nonlinear system $\dot{\mathbf{x}} = \mathbf{f}(\mathbf{x})$ *is locally exponentially stable about* $\mathbf{x} = \mathbf{0}$*.*

Based on Theorem 4.2, for the nonlinear system (34)–(38) describing vascular growth, the 2-state system $(\Delta\dot{M}, \Delta y)$ is locally exponentially stable, i.e., locally $\dot{M} \to 0$ and $y \to y_h$ exponentially.

It can be noted that the stabilizing condition (73) for $(\Delta\dot{M},\ \Delta y)$ is the same as the one in (61) derived from the degenerate linear system for $(\Delta M,\ \Delta r)$. (The additional criterion $\alpha > 0$ from considering Δy is automatically satisfied by definition.) However, the above analysis is necessary to establish *exponential stability* for the linear system, which enables the extrapolation to the original nonlinear system. On the other hand, we would like to establish the behavior of the mass density M, as opposed to its time derivative $\dot{M}$. This can be achieved however by noticing that, due to local exponential stability of $\Delta\dot{M}$, there exist constants $a > 0$ and $b > 0$ such that

$$\|\Delta\dot{M}\| \le be^{-at}, \quad \forall\ t > 0 \tag{76}$$

within a local neighborhood. To obtain a norm estimation of mass density $M(t)$, we first integrate $\Delta\dot{M}$ from 0 to t

$$\Delta M(t) = \Delta M(0) + \int_0^t \Delta\dot{M} dt\ . \tag{77}$$

Taking the norm for the above equation and applying the triangle inequality gives

$$\begin{aligned} \|\Delta M(t)\| &\le \|\Delta M(0)\| + \int_0^t \|\Delta\dot{M}\| dt \\ &\le \|\Delta M(0)\| + b\int_0^t e^{-at} dt \\ &= \|\Delta M(0)\| + b\,\frac{1-e^{-at}}{a} \\ &\le \|\Delta M(0)\| + \frac{b}{a}\ . \end{aligned} \tag{78}$$

Applying the triangle inequality again, an estimation of the norm of $M(t)$ for the nonlinear system can be obtained as

$$\|M(t)\| = \|M_h + \Delta M(t)\| \le \|M_h\| + \|\Delta M(t)\| \le \|M_h\| + \|\Delta M(0)\| + \frac{b}{a} \le C < \infty\ . \tag{79}$$

Similarly, if we construct the 2-state system of $(\dot{\Delta r}, \Delta y)$ and apply the same analysis above, we can obtain

$$\|r(t)\| < \infty \tag{80}$$

under same stabilizing condition (73).

4.4 Asymptotic stability for wall tension $\sigma(t)$

By taking the time derivative of (38), we can obtain the linearized ODE for the time evolution of wall tension deviation

$$\begin{aligned} \frac{d}{dt}\Delta\sigma(t) &= \frac{\rho P}{R}\left[\frac{2r(t)}{M(t)}\dot{r}(t) - \frac{r^2(t)}{M^2(t)}\dot{M}(t)\right] \\ &\approx \left[\frac{1}{k_h}\left[2\alpha - \frac{2k_g r_h^2 \rho P}{RM_h}\right] - \frac{k_g \rho P r_h^2}{RM_h}\right]\Delta\sigma \\ &= [A + D]\Delta\sigma\ , \end{aligned} \tag{81}$$

which implies that stability criteria (73) also ensures the exponential stability for wall tension deviation, i.e.

$$\lim_{t\to\infty} \Delta\sigma(t) = 0 \, . \tag{82}$$

4.5 Summary of stability conclusions

When the following stability conditions are satisfied,

$$k_g > \frac{\alpha R M_h}{\rho P r_h^2} \left[\frac{1}{1 + \frac{E M_h}{2\rho P r_h}} \right] \triangleq k_{cr}, \qquad \alpha > 0$$

the states $r(t)$, $M(t)$, $y(t)$ and $\sigma(t)$ for the nonlinear system (34–36) have the following stability behavior about the homeostatic states

$$\begin{aligned} \|r(t)\| < \infty \quad &\Rightarrow \quad r(t) \text{ is neutrally stable ;} \\ \|M(t)\| < \infty \quad &\Rightarrow \quad M(t) \text{ is neutrally stable ;} \\ y(t) \to y_h \quad &\Rightarrow \quad y(t) \text{ is asymptotically stable ;} \\ \sigma(t) \to \sigma_h \quad &\Rightarrow \quad \sigma(t) \text{ is asymptotically stable ,} \end{aligned} \tag{83}$$

Thus, stability analysis shows that even when the stability criteria (73) is satisfied, only σ and y will converge to corresponding homeostatic values as $t \to \infty$ while M and r will only stay bounded but not necessarily converge to the original homeostatic values. This matches observation in [4, 28] that in stable aneurysm expansion cases, only wall tension σ is able to recover the homeostatic value while the geometry and mass density cannot return to the original homeostatic states.

5 Numerical Experiments

In this section we simulate the aneurysm expansion based on the system of nonlinear differential equations (34–38). Material constants and geometric constants used in the simulations are listed in Table 1. All simulations were done within *Simulink*. In all simulations, pathological G&R is triggered by introducing 50% initial mass loss of vascular constituents as in [4, 13]. As mentioned above, in order to eliminate dependence of the problem on spatial coordinates and obtain a system of ordinary differential equations, uniform initial mass loss is considered.

Based on the stabilizing criteria (73) and the given G&R parameters listed in Table 1, the critical value of the growth feedback constant is $k_{cr} = 2.1 \times 10^{-6}$. The stabilizing condition (73) indicates that aneurysm expansion is stable when $k_g > k_{cr}$ while the aneurysm expansion is unstable when $k_g \leq k_{cr}$. To test this, four scenarios of pathological G&R are simulated with different values of the growth feedback constant: Case (1) $k_g = 1.5 \times 10^{-6}$, Case (2) $k_g = 3.0 \times 10^{-6}$, Case (3) $k_g = 5.0 \times 10^{-6}$, Case (4) $k_g = 7.0 \times 10^{-6}$. The time evolution of the state variables of aneurysm expansion, mass density $M(t)$, vessel radius $r(t)$, generalized stiffness $y(t)$ and wall tension $\sigma(t)$, were recorded and plotted in Figure 2. The simulation results show that when $k_g > k_{cr}$ (Case 2–4), vascular expansion is stable. In these three stable cases, we observed that generalized stiffness $y(t)$ and wall tension $\sigma(t)$ converge to the corresponding homeostatic states asymptotically while mass density $M(t)$ and vessel radius $r(t)$ only exhibit neutral stability, i.e., the values of the states remain bounded. In Case 1, where $k_g < k_{cr}$, vessel radius $r(t)$ and wall tension $\sigma(t)$ both increase

Table 1: Mechanical, geometric and G&R kinetic constants [3, 29]

$\alpha = 2.3$	$E = 1.9 \times 10^6 Pa$	$P = 13332\ Pa$	$r_h = 0.0075\ m$
$G_h = 1.05$	$M_h = 1.0904\ kg/m^2$	$\sigma_h = 1.01 \times 10^5\ Pa$	$\rho = 1050\ kg/m^3$

unboundedly, which indicates unstable vascular expansion. Also observed is that the larger the value of k_g, the faster the states converge to the steady states.

We also simulated four cases with increased stiffness E to study the influence of vessel stiffness on aneurysm expansion. The value of stiffness was increased to $E = 3.8 \times 10^6$ Pa while all other parameters remained unchanged. For this value of E, the critical value for the growth feedback constant is $k_{cr} = 1.0 \times 10^{-6}$. Four scenarios were considered, with Case (1) $k_g = 1.5 \times 10^{-6}$, Case (2) $k_g = 3.0 \times 10^{-6}$, Case (3) $k_g = 5.0 \times 10^{-6}$, Case (4) $k_g = 7.0 \times 10^{-6}$, and the time course of the four state variables are plotted in Figure 3. For the elevated value of stiffness E, all four cases satisfy the stabilizing condition $k_g > k_{cr}$ and all four cases obtain stable vascular expansion, including the case of $k_g = 1.5 \times 10^{-6}$ that was unstable for the normal value of stiffness E.

Lastly, we simulated four cases considering an increase of vascular constituent decay constant $\alpha = 4.6$. This corresponds to an increase of turnover rate of vascular constituents, e.g., collagen and smooth muscle. For this scenario, the critical value for the growth feedback constant was $k_{cr} = 4.1 \times 10^{-6}$. The time evolution of the four state variables for Case (1) $k_g = 1.5 \times 10^{-6}$, Case (2) $k_g = 3.0 \times 10^{-6}$, Case (3) $k_g = 5.0 \times 10^{-6}$, Case (4) $k_g = 7.0 \times 10^{-6}$ are plotted in Figure 4. With the elevated value of the decaying constant, Cases (3) and (4) satisfies the stabilizing criteria while Cases (1) and (2) do not. Figure 4 shows that only in Cases (3) and (4), vessel radius remains bounded and wall tension converges to the homeostatic value, while in Case (1) and (2) G&R results in unbounded vascular expansion. Case (2), which is stable under the normal conditions, is destabilized due to elevated decaying constant α.

6 Discussion

While prior works [13, 2, 23, 28] have focused on computationally investigating aneurysm expansion based on the constrained mixture theory of vascular G&R, we herein provide an analytical study of the stability properties of this model. Under appropriate assumptions, the constrained mixture model was used to develop a nonlinear ODE system governing vascular growth, and stability criteria (73) were derived for growth about the homeostatic state in terms of G&R kinetic parameters, geometric quantities and material properties.

To obtain stability conclusions for the nonlinear system about the homeostatic state, we first linearized the nonlinear equations. The resulting linearization was shown to be degenerate, failing to determine the stability of the original nonlinear system. Indeed, the neutral stability property of vascular G&R observed in prior theoretical [9, 10] and computational [28] studies is due to this degeneracy, however stability properties for the original (nonlinear) system had not previously been established rigorously. To address this problem, we consider the 2-state subsystem $(\Delta M, \Delta y)$, in which Δr was eliminate due to its linear dependence on ΔM. While the resulting equation for ΔM was non-homogenous, it was homogenized by taking its time derivative. The resulting dynamics for $(\Delta \dot{M}, \Delta y)$ was made exponentially stable by setting its eigenvalues to be negative, by which local exponential stability of the mass density rate $\Delta \dot{M}$ and generalized stiffness Δy for the nonlinear system were established. Using the local exponential stability of $\Delta \dot{M}$ and the triangle

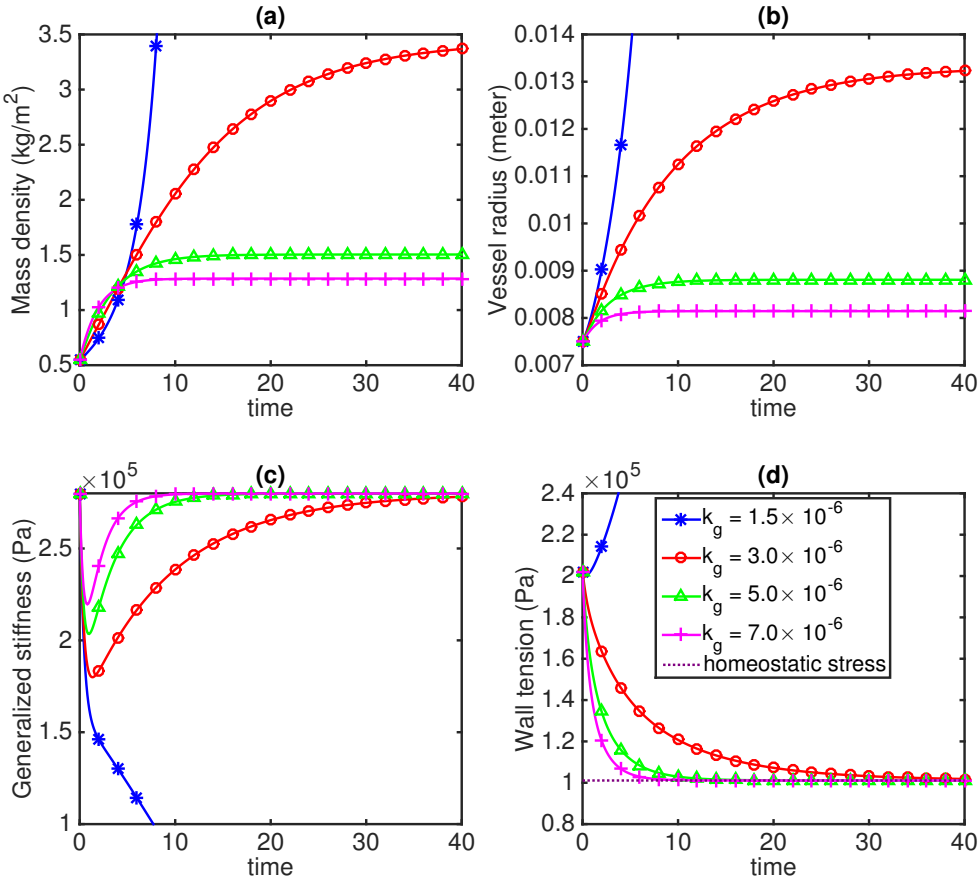

Figure 2: Time evolution of vessel properties ($M(t)$, $r(t)$, $y(t)$ and $\sigma(t)$) using various values of growth feedback constant k_g from solving the nonlinear evolution equations. The corresponding critical value for the growth feedback constant is $k_{cr} = 2.1 \times 10^{-6}$.

inequality, neutral stability of the mass density $M(t)$ for the nonlinear system was established. Similar arguments imply that the vessel radius $r(t)$ is neutrally stable and wall tension $\sigma(t)$ is exponentially stable for the nonlinear system.

When converting the integral equation (21) for the vessel radius r to a non-delayed ODE, we derived an extended state y defined by (31). The meaning of y is discussed here. Consider the vascular force in the circumferential direction

$$T_\theta(t) = Pr(t) = R \int_0^t \frac{m(\tau)}{\rho} q(t-\tau) E \left[G_h \frac{r(t)}{r(\tau)} - 1 \right] \frac{G_h}{r(\tau)} d\tau \, . \tag{84}$$

Now take the first variation of the above equation corresponding to a snapshot of the G&R process.

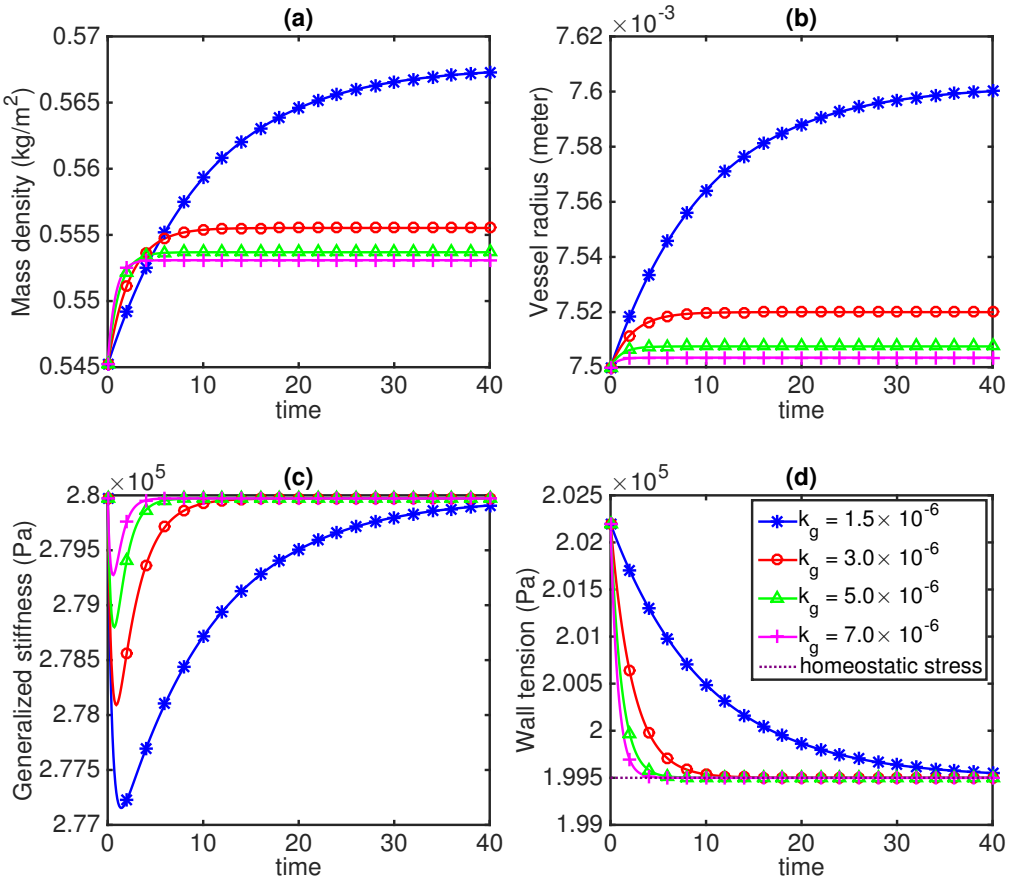

Figure 3: Time evolution of vessel properties ($M(t)$, $r(t)$, $y(t)$ and $\sigma(t)$) using various values of growth feedback constant k_g for increased arterial stiffness **E**. The corresponding critical value for the growth feedback constant is $k_{cr} = 1.0 \times 10^{-6}$.

Since $q(t)$ is a known function of t and time is fixed when taking the variation, δq and δt are both equal to zero. The only two functions that have non-zero first variation are δT_θ and δr, and

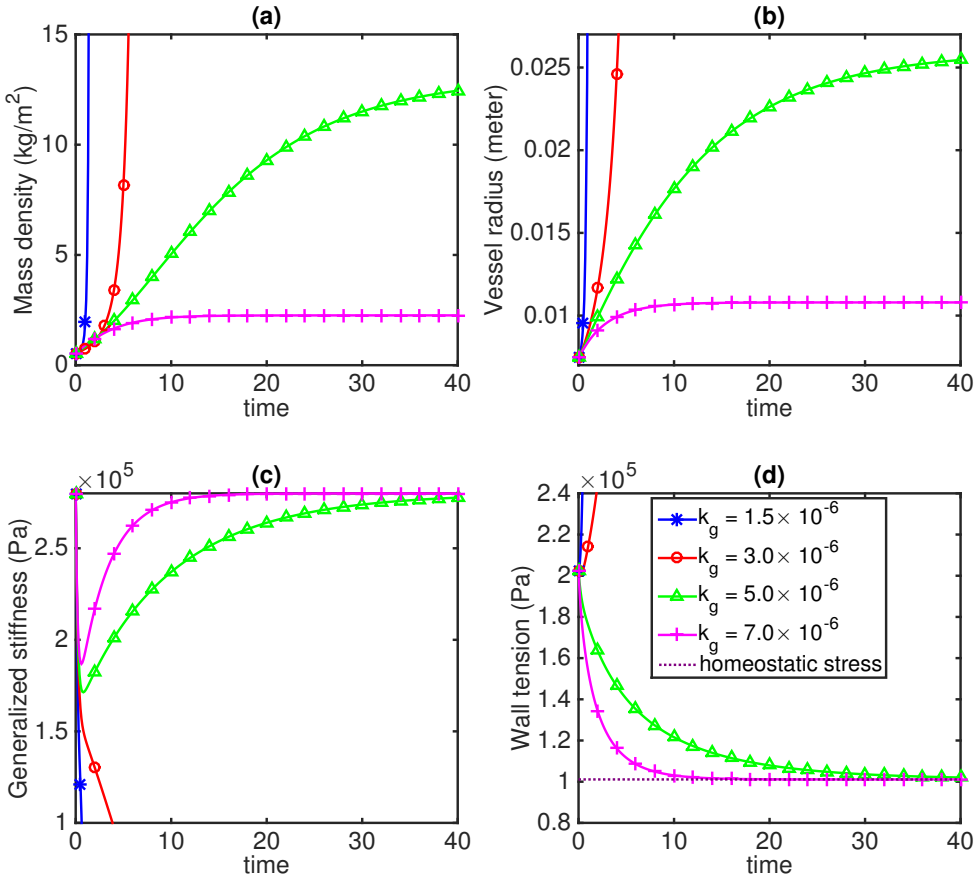

Figure 4: Time evolution of vessel properties ($M(t)$, $r(t)$, $y(t)$ and $\sigma(t)$) using various values of growth feedback constant k_g for increased decay constant α. The corresponding critical value for the growth feedback constant is $k_{cr} = 4.1 \times 10^{-6}$

therefore, the equation is reduced into the following form

$$\begin{aligned}
\delta T_\theta &= \delta\left[R\int_0^t \frac{m(\tau)}{\rho} q(t-\tau) E\left[G_h \frac{r(t)}{r(\tau)} - 1\right]\frac{G_h}{r(\tau)} d\tau\right] \\
&= R\int_0^t \frac{m(\tau)}{\rho} q(t-\tau) E\delta\left[G_h \frac{r(t)}{r(\tau)} - 1\right]\frac{G_h}{r(\tau)} d\tau \\
&= R\int_0^t \frac{m(\tau)}{\rho} q(t-\tau) E\frac{G_h^2}{r^2(\tau)} d\tau \cdot \delta r \\
&= y(t)\cdot\delta r\,. \qquad (85)
\end{aligned}$$

Therefore, the extended state y can be defined as the ratio of variations of stress and strain in circumferential direction, multiplied by a constant $\frac{R}{h}$,

$$y = \frac{\delta T_\theta}{\delta r} = \frac{\delta T_\theta / h}{\delta r / R} \frac{R}{h} = \frac{\delta \sigma_\theta}{\delta \epsilon_\theta} \frac{R}{h} \, . \tag{86}$$

This implies that y physically represents a generalized stiffness resisting radial expansion for the mixture of vascular constituents. In our study we only consider one species of vascular constituents aligned in the circumferential direction for simplicity. However, within one constituent family, constituents produced at different times τ forms a *mixture* of constituents that possess different natural configurations. It is straightforward to extend the theory to a mixture model with multiple species, however cases of asymmetric expansion would require more careful analysis of the associated kinematics.

The derived stability criteria for the nonlinear system were verified by numerical simulations. As shown in Figure 2, for the three cases (Case 2-4) satisfying the derived stability criteria, only the generalized stiffness y and the wall tension σ converge to their homeostatic values, while vessel radius r and mass density M only remain bounded (they do not converge to specific homeostatic values). These results from numerically integrating the nonlinear evolution equations are consistent with the stability conclusions obtained from the presented theoretical analysis. When the system is stable, only y and σ exhibit local exponential stability while r and M exhibit neutral stability. It is interesting to note that these convergence behaviors match with prior observations from computational studies in idealized [4, 5] and patient-specific [28] geometries, where less restrictive modeling assumptions were employed than those used to develop the theoretical model herein. Moreover, we note that while the theoretical analysis only implies *local* stability properties about the homeostatic state, the numerical experiments considered *large* deviations from the homeostatic state; nonetheless identical stability properties were observed as predicted by the theoretical model.

For the numerical experiments, pathological G&R was triggered by introducing an initial mass loss to the vessel wall. This caused an immediate weakening of vessel, as reflected in the initial drop of the generalized stiffness y (see Figure 2c). However, for the three stable cases (Case 2-4), after the initial drop due to mass loss, the generalized stiffness y recovered back to the homeostatic value. This is because when $k_g > k_{cr}$, thickening of vessel wall caused by stress mediated growth is fast enough to compensate the natural expansion caused by the initial mass loss and natural turnover of vascular constituent. On the other hand, for Case 1, $k_g \leq k_{cr}$, and the stress mediated growth (feedback) is not strong enough to compensate for the weakening of the vessel and natural turnover. Therefore, expansion proceeds with continuous increase of vessel radius r and wall tension σ.

Based on the stabilizing criteria (73), the stability of vascular expansion depends on growth parameters (k_g, α) and material properties ($\mathbf{E}$, ρ). To understand how these factors influence the stability behavior, we first increased the material stiffness E holding all other parameters at their nominal values. The simulation results (Figure 3) show that, when stiffness $\mathbf{E}$ is doubled, all four values of the feedback growth constant k_g are stable, including the case $k_g = 1.5 \times 10^{-6}$ which was originally not stable. This can be seen from the definition of the critical value k_{cr}

$$k_{cr} \triangleq \frac{\alpha R M_h}{\rho P r_h^2} \left[\frac{1}{1 + \frac{E M_h}{2 \rho P r_h}} \right] \, . \tag{87}$$

When material stiffness E increases, k_{cr} decreases and stabilizing criterion will be easier to satisfy. This result that increased arterial stiffness may have a stabilizing effect matches observations in [10,

21]. We note however that in previous clinical studies [11, 20], it has been observed that increased wall stiffness correlates with the occurrence of aortic aneurysm. However, increased vessel wall stiffness may be a consequence of the disease than a direct cause. Alternatively, other factors may be at play in vivo that are not considered in the present modeling.

We also sought to understand the influence of growth parameters (k_g, α). The constant α defines the rate of vascular constituent turnover. When α was increased, the results in Figure 4 demonstrate a destabilizing behavior. Namely, Case 2 ($k_g = 3.0 \times 10^{-6}$) that was stable for the nominal parameter set led to unstable expansion. Again, this trend can be anticipate from (87). As α is increased, the critical value for the feedback growth constant also increases, and the cases of $k_g = 1.5 \times 10^{-6}$ and $k_g = 3.0 \times 10^{-6}$ fail to satisfy the stabilizing condition. Prior studies [22, 1] have observed increased collagen turnover in abdominal aortic aneurysms and ruptured abdominal aortic aneurysms. Additionally, [12] found that the collagen turnover is significantly more rapid in patients with risk factors for aneurysm formation/rupture, such as smoking or hypertension. These observations are consistent with the theoretical and computational analyses here that increased decay constant α can destabilize the vascular G&R process.

While we assumed (mean) blood pressure to be constant in our analysis, we here consider the effect of increased blood pressure (hypertension) on the stability of vascular G&R. Based on the stabilizing criterion (87), an increase of mean blood pressure P will cause a decrease of the critical value k_{cr}, which indicates that hypertension acts as a stabilizing factor. However, this is inconsistent with evidence that hypertension is a risk factor for aneurysm growth and rupture [8]. It is important to notice that (40) holds true only when P denotes the pressure producing the homeostatic hoop stress σ_h when $M = M_h$ and $r = r_h$. Let us denote the homeostatic pressure as P_h. In order to study the influence of mean blood pressure on the stability of aneurysm expansion, we need to consider a deviation from the homeostatic pressure. Thus, for a general pressure P in (21), we assume

$$P = P_h + \Delta P \tag{88}$$

where ΔP is a small pressure deviation and $P_h = \frac{E[G_h - 1]M_h}{\rho r_h}$ based on (40). Note that we here only consider a constant change of pressure, i.e. ΔP is independent of time. After the same procedure of linearization, the 3-state linear system equation becomes

$$\frac{d}{dt}\begin{bmatrix} \Delta r \\ \Delta M \\ \Delta y \end{bmatrix} = \begin{bmatrix} \frac{1}{k_h}\left[\alpha - \frac{k_g \rho P_h r_h^2}{R M_h}\right]\left[2\Delta r - \frac{r_h}{M_h}\Delta M + \frac{r_h}{P_h}\Delta P\right] \\ \frac{k_g \rho P_h r_h}{R}\left[2\Delta r - \frac{r_h}{M_h}\Delta M + \frac{r_h}{P_h}\Delta P\right] \\ -\frac{k_2 M_h}{r_h^3}\left[\alpha - \frac{k_g \rho P_h r_h^2}{R M_h}\right]\left[2\Delta r - \frac{r_h}{M_h}\Delta M + \frac{r_h}{P_h}\Delta P\right] - \alpha\left[\Delta y - \frac{k_2 M_h}{r_h^2 P_h}\Delta P\right] \end{bmatrix} \tag{89}$$

If we set the new deviation variable for generalized stiffness $y(t)$ as

$$\overline{\Delta y} \triangleq \Delta y - \frac{k_2 M_h}{r_h^2 P_h}\Delta P \,, \tag{90}$$

a similar 2-state homogeneous system can be obtained with respect to $(\Delta\dot{M}, \overline{\Delta y})$ by making use of the same linear relation (66)

$$\frac{d}{dt}\begin{bmatrix} \Delta\dot{M} \\ \overline{\Delta y} \end{bmatrix} = \begin{bmatrix} \frac{k_g \rho P_h r_h}{R}\left[2B_1 - \frac{r_h}{M_h}\right] & 0 \\ B_3 & -\alpha \end{bmatrix} \times \begin{bmatrix} \Delta\dot{M} \\ \overline{\Delta y} \end{bmatrix} . \tag{91}$$

Note that the coefficient matrix of the above 2-state system is the same as that of (70), except the pressure P is now replaced by the homeostatic pressure P_h. Therefore, the same stabilizing condition is obtained as follow

$$k_g > \frac{\alpha R M_h}{\rho P_h r_h^2}\left[\frac{1}{1+\frac{EM_h}{2\rho P_h r_h}}\right] \triangleq k_{cr}, \quad \alpha > 0\ . \tag{92}$$

Substituting $P_h = \frac{E[G_h-1]M_h}{\rho r_h}$ into the above inequality yields

$$k_{cr} = \frac{\alpha}{EG_h\left[G_h-\frac{1}{2}\right]} \approx 1.732\frac{\alpha}{E} \tag{93}$$

which is independent of the pressure deviation ΔP. Therefore, from the linear analysis, the stability of vascular G&R is independent of mean blood pressure.

However, the above does not imply that blood pressure does not affect solution behavior. Note that $B_1 > 0$ if

$$k_g < \frac{\alpha R M_h}{\rho P r_h^2} = \frac{\alpha}{EG_h\left[G_h-1\right]} \approx 19.048\frac{\alpha}{E} \gg k_{cr}\ . \tag{94}$$

We here assume the normal range of the value for k_g is around k_{cr}, which is much less than $19.048\frac{\alpha}{E}$. Therefore, B_1 is always positive. Based on the linear relation between $\Delta r(t)$ and $\Delta M(t)$ in (66), and the second equation of (89) ,

$$\frac{d}{dt}\Delta M = \lambda_1 \Delta M + \frac{k_g \rho P_h r_h}{R}\left[2B_2 + \frac{r_h}{P_h}\Delta P\right]\ , \tag{95}$$

where

$$\lambda_1 = \frac{k_g \rho P_h r_h}{R}\left[2B_1 - \frac{r_h}{M_h}\right] = 2EG_h\left[G_h-1\right]\left[G_h-\frac{1}{2}\right]\left[k_{cr}-k_g\right] \tag{96}$$

The solution to the above equation is

$$\Delta M(t) = B_4 e^{\lambda_1 t} + \frac{k_g \rho P_h r_h}{-\lambda_1 R}\left[2B_2 + \frac{r_h}{P_h}\Delta P\right]\ , \tag{97}$$

where B_4 is a constant that depends on the initial condition. Based on the linear relation (66), the solution for radius change $\Delta r(t)$ is

$$\Delta r(t) = B_1 B_4 e^{\lambda_1 t} + \frac{B_1 k_g \rho P_h r_h}{-\lambda_1 R}\left[2B_2 + \frac{r_h}{P_h}\Delta P\right] + B_2\ . \tag{98}$$

The stability of the solution is determine by the exponential term $e^{\lambda_1 t}$. Since ΔP does not influence the λ_1, it does not influence the stability of the system. However, ΔP does influences the particular solutions for $\Delta M(t)$ and $\Delta r(t)$. Therefore, ΔP will cause a shift of the steady states (if they exist), but not the stability of the system.

In the case of stable vascular G&R ($k_g > k_{cr}$, $\lambda_1 < 0$),

$$\Delta M(t \to +\infty) = \frac{k_g \rho P_h r_h}{-\lambda_1 R}\left[2B_2 + \frac{r_h}{P_h}\Delta P\right]\ , \tag{99}$$

$$\Delta r(t \to +\infty) = \frac{B_1 k_g \rho P_h r_h}{-\lambda_1 R} \left[2B_2 + \frac{r_h}{P_h} \Delta P \right] + B_2 \ . \tag{100}$$

Therefore, if ΔP increases, it will cause the final mass density to increase. Indeed, vascular mass density needs to increase in order to balance the increased pressure and maintain the homeostatic stress σ_h. Also (90) shows that increased ΔP causes an increased shift of Δy. This also corresponds to the fact that the overall stiffness of the vascular mixture needs to increase to compensate for the increased pressure. Similarly, due to the positiveness of B_1, increased ΔP will cause the increased shift of the final steady state radius. In comparison with prior studies, it has similarly been shown that hypertension (i.e., increased ΔP) does not change the stability of expansion, however it does increase the thickness (proportional to mass density) of vessel wall [27, 7] and the final size of the aneurysm. Also based on the first equation of (89), hypertension increases the vessel expansion rate $\dot{\Delta r}$, which is consistent with prior clinical findings [15], regardless of whether the expansion is stable or not. The analysis above considers only the direct influence of hypertension on stability of vascular G&R. However, hypertension may change stability through other factors not considered. For example, [19] indicate that collagen turnover in aorta and arteries are increased under hypertension. This corresponds to increased of α in our analysis, which is a destabilizing factor for vascular G&R.

7 Conclusion

Herein a theoretical framework describing aneurysm expansion is derived based on vascular G&R theory. A system of nonlinear ordinary differential equations are obtained from the integral equations of constrained mixture theory for G&R to characterizing vascular expansion. Based on stability analysis for the nonlinear system, we derived a stabilizing condition for aneurysm expansion in terms of material properties (E, ρ), G&R parameters (k_g, α), geometry (R, r_h). From the stability analysis, in the stable expansion case, only wall tension σ and generalized stiffness y exhibit convergence to the corresponding homeostatic values while vessel radius r and mass density of vascular constituents only remain bounded without converging to any specific values. These theoretical stability conclusions were verified by numerical simulations. Additionally, we also studied the effect of increased stiffness E and increased decaying constant α on the stability of aneurysm expansion. Both the theoretical analysis and numerical simulation show that increased stiffness a stabilizing effect of aneurysm expansion while increased decaying constant (i.e., increased turnover rate of vascular constituents) is a destabilizing effect. Indeed, previous work on aneurysm expansion is more focused on applying computational techniques and clinic estimation of aneurysm rupture risk is usually based only on geometry (e.g. vascular radius). However, in this work, we focused on theoretical analysis, related aneurysm rupture to the stability of aneurysm expansion, and obtained a more comprehensive conditions for stable aneurysm expansion involving consideration of different aspects including material properties (E, ρ), G&R parameters (k_g, α) and hypertensive effect.

References

[1] H Abdul-Hussien, RGV Soekhoe, E Weber, H Jan, R Kleemann, A Mulder, JH Van Bockel, R Hanemaaijer, and JHN Lindeman. Collagen degradation in the abdominal aneurysm: a conspiracy of matrix metalloproteinase and cysteine collagenases. *The American Journal of Pathology*, 170(3):809–817, 2007.

[2] P Aparício, A Mandaltsi, J Boamah, H Chen, A Selimovic, M Bratby, R Uberoi, Y Ventikos, and PN Watton. Modelling the influence of endothelial heterogeneity on the progression of arterial disease: Application to abdominal aortic aneurysm evolution. *International Journal for Numerical Methods in Biomedical Engineering*, 30(5):563–586, 2014.

[3] GM Austin, W Schievink, and R Williams. Controlled pressure-volume factors in the enlargement of intracranial aneurysms. *Neurosurgery*, 24(5):722–730, 1989.

[4] S Baek, KR Rajagopal, and JD Humphrey. Competition between radial expansion and thickening in the enlargement of an intracranial saccular aneurysm. *Journal of Elasticity*, 80(1-3):13–31, 2005.

[5] S Baek, KR Rajagopal, and JD Humphrey. A theoretical model of enlarging intracranial fusiform aneurysms. *Journal of Biomechanical Engineering*, 128(1):142–149, 2006.

[6] DK Bogen and TA McMahon. Do cardiac aneurysms blow out? *Biophysical Journal*, 27(2):301, 1979.

[7] ML Bots, A Hofman, AM de Bruyn, PT De Jong, and DE Grobbee. Isolated systolic hypertension and vessel wall thickness of the carotid artery. the rotterdam elderly study. *Arteriosclerosis, Thrombosis, and Vascular Biology*, 13(1):64–69, 1993.

[8] E Choke, G Cockerill, WRW Wilson, S Sayed, J Dawson, I Loftus, and MM Thompson. A review of biological factors implicated in abdominal aortic aneurysm rupture. *European Journal of Vascular and Endovascular Surgery*, 30(3):227–244, 2005.

[9] CJ Cyron and JD Humphrey. Vascular homeostasis and the concept of mechanobiological stability. *International journal of engineering science*, 85:203–223, 2014.

[10] CJ Cyron, JS Wilson, and JD Humphrey. Mechanobiological stability: a new paradigm to understand the enlargement of aneurysms? *Journal of The Royal Society Interface*, 11(100):20140680, 2014.

[11] JM Dijk, Y Van Der Graaf, DE Grobbee, JD Banga, ML Bots, et al. Increased arterial stiffness is independently related to cerebrovascular disease and aneurysms of the abdominal aorta the second manifestations of arterial disease (smart) study. *Stroke*, 35(7):1642–1646, 2004.

[12] N Etminan, R Dreier, BA Buchholz, K Beseoglu, P Bruckner, C Matzenauer, JC Torner, RD Brown, H Steiger, D Hänggi, et al. Age of collagen in intracranial saccular aneurysms. *Stroke*, 45(6):1757–1763, 2014.

[13] AC Figueroa, S Baek, CA Taylor, and JD Humphrey. A computational framework for fluid–solid-growth modeling in cardiovascular simulations. *Computer Methods in Applied Mechanics and Engineering*, 198(45):3583–3602, 2009.

[14] GA Holzapfel, TC Gasser, and RW Ogden. A new constitutive framework for arterial wall mechanics and a comparative study of material models. *Journal of elasticity and the Physical Science of Solids*, 61(1-3):1–48, 2000.

[15] Y Huang, P Gloviczki, AA Duncan, M Kalra, TL Hoskin, GS Oderich, MA McKusick, and TC Bower. Common iliac artery aneurysm: expansion rate and results of open surgical and endovascular repair. *Journal of Vascular Surgery*, 47(6):1203–1211, 2008.

[16] JD Humphrey. Towards a theory of vascular growth and remodeling. In GA Holzapfel and RW Ogden, editors, *Mechanics of Biological Tissue*, pages 3–15. Springer Berlin Heidelberg, 2006.

[17] JD Humphrey. *Cardiovascular Solid Mechanics: Cells, Tissues, and Organs*. Springer-Verlag New York, 2013.

[18] JD Humphrey and KR Rajagopal. A constrained mixture model for growth and remodeling of soft tissues. *Mathematical Models and Methods in Applied Sciences*, 12(03):407–430, 2002.

[19] R Nissen, GJ Cardinale, and S Udenfriend. Increased turnover of arterial collagen in hypertensive rats. *Proceedings of the National Academy of Sciences*, 75(1):451–453, 1978.

[20] ME Safar, MF O'Rourke, and ED Frohlich. *Blood Pressure and Arterial Wall Mechanics in Cardiovascular Diseases*. Springer, 2014.

[21] G Satha, SB Lindström, and A Klarbring. A goal function approach to remodeling of arteries uncovers mechanisms for growth instability. *Biomechanics and Modeling in Mechanobiology*, 13(6):1243–1259, 2014.

[22] J Satta, T Juvonen, K Haukipuro, M Juvonen, and MI Kairaluoma. Increased turnover of collagen in abdominal aortic aneurysms, demonstrated by measuring the concentration of the aminoterminal propeptide of type iii procollagen in peripheral and aortal blood samples. *Journal of Vascular Surgery*, 22(2):155–160, 1995.

[23] A Sheidaei, SC Hunley, S Zeinali-Davarani, LG Raguin, and S Baek. Simulation of abdominal aortic aneurysm growth with updating hemodynamic loads using a realistic geometry. *Medical Engineering & Physics*, 33(1):80–88, 2011.

[24] A Valentin and JD Humphrey. Evaluation of fundamental hypotheses underlying constrained mixture models of arterial growth and remodelling. *Philosophical Transactions of the Royal Society of London A: Mathematical, Physical and Engineering Sciences*, 367(1902):3585–3606, 2009.

[25] F Verhulst. *Nonlinear Differential Equations and Dynamical Systems*. Springer-Verlag Berlin Heidelberg, 1996.

[26] PN Watton, NB Raberger, GA Holzapfel, and Y Ventikos. Coupling the hemodynamic environment to the evolution of cerebral aneurysms: computational framework and numerical examples. *Journal of Biomechanical Engineering*, 131(10):101003, 2009.

[27] H Wolinsky. Long-term effects of hypertension on the rat aortic wall and their relation to concurrent aging changes: morphological and chemical studies. *Circulation Research*, 30(3):301–309, 1972.

[28] J Wu and SC Shadden. Coupled simulation of hemodynamics and vascular growth and remodeling in a subject-specific geometry. *Annals of Biomedical Engineering*, 43(7):1543–1554, 2015.

[29] S Zeinali-Davarani, A Sheidaei, and S Baek. A finite element model of stress-mediated vascular adaptation: application to abdominal aortic aneurysms. *Computer Methods in Biomechanics and Biomedical Engineering*, 14(9):803–817, 2011.